

# Activation of Small GTPase Rho Is Required for Autocrine Motility Factor Signaling<sup>1</sup>

Soichi Tsutsumi, Suresh K. Gupta, Victor Hogan, John G. Collard, and Avraham Raz<sup>2</sup>

Metastasis Research Program, Karmanos Cancer Institute and the Department of Pathology, Wayne State University School of Medicine, Detroit, Michigan 48201 [S. T., S. K. G., V. H., A. R.], and Netherlands Cancer Institute, Division of Cell Biology, 1066 CX Amsterdam, the Netherlands [J. G. C.]

## ABSTRACT

The hallmark of tumor metastasis is the dissemination of cells from the primary growth site to distant organs. Autocrine motility factor (AMF), a tumor-associated C-X-X-C cytokine, the ligand for a unique 78 kDa seven transmembrane receptor, is a potent simulator of cell motility, a process that is a prerequisite for tumor progression and metastasis. Because little is known about AMF-dependent signaling, we sought to study whether AMF signaling involves family members of the Rho-like GTPases. AMF stimulation of human melanoma cells resulted in stress-fiber formation, concomitant with up-regulation and activation of both RhoA and Rac1 expression with no apparent changes in the expression level or activation state of Cdc42. Treatment of the cells with C3 exoenzyme before AMF stimulation inhibited both the formation of stress-fiber-like structures and the activation of RhoA. In addition, both c-Jun NH<sub>2</sub>-terminal kinase 1 and c-Jun NH<sub>2</sub>-terminal kinase 2 were simultaneously activated by AMF, supporting the notion that they are involved in the signaling pathway of RhoA. We thus conclude that AMF signaling shares a similar pathway to previously established paracrine factors signaling involving cytoskeletal rearrangement and morphological alterations mediated by the small RhoA-like GTPases.

## INTRODUCTION

Cell migration is an essential aspect of various normal and pathological processes, including embryonic development, wound healing, inflammation, and tumor cell invasion and metastasis (1–4). An AMF<sup>3</sup> is a tumor-secreted polypeptide with apparent molecular mass of 55 kDa and 64 kDa under nonreducing and reducing conditions, respectively, originally identified by its ability to induce the migration of the AMF-producing tumor cells via a receptor-mediated pathway (5, 6). Molecular cloning and sequencing have identified AMF as PHI (6, 7), the cytokine NLK (8), the differentiation inducer maturation factor (7–12), and more recently as the myofibril-bound serine proteinase inhibitor (13). PHI catalyzes the interconversion of D-fructose-6-phosphate, and D-glucose-6-phosphate (14) is a glycolytic enzyme and therefore a housekeeping gene transcribed in all cells, which exhibit extracellular alternative functions, including cytokine and growth factor activities. The molecule has a unique motif of C-X-X-C (6, 7) shared with the macrophage-stimulating factor (11) and its receptor is a seven transmembrane glycoprotein similar in structure to the chemokines (C-X-C, C-X-X-C molecules) receptor, albeit of a different gene family. It is well established that PHI is present extracellularly. Elevated serum PHI levels are used as a tumor marker in patients with colorectal, breast, lung, kidney, and gastrointestinal carcinomas, and relative activities are correlated with the development

of metastases (15–20). The overexpression of c-MYC oncoprotein deregulates the glycolysis and results in elevated levels of several enzymes of the glucose metabolic pathway, including PHI (21). Surprisingly, PHI/AMF/NLK/maturation factor was recently found to exhibit an unrelated function as a specific inhibitor of myofibril-bound serine proteinase(s) (13). Furthermore, PHI was implicated as a self-pathogenic antigen responsible for the onset of rheumatoid arthritis and to be localized within the synovium (22, 23).

Analysis of the signaling pathway of AMF in tumor cells has revealed that it involves receptor phosphorylation (6) and activation of cell motility, which is mediated by a pertussis toxin-sensitive G protein (24). It is also involved in the activation of phospholipase(s) and the inositol cycle (25) with two downstream key components: 12-lipoxygenases and protein kinase C (26). AMF was also shown to induce dephosphorylation of cellular protein on tyrosine residues, including focal adhesion kinase, together with rearrangement of focal adhesion components. Because stimulation of resting cells to migration involves an extensive reorganization of the cytoskeleton, we therefore investigated the possible role of Rho-like GTPases in AMF signaling as the cytoskeletal alterations are associated with a migratory phenotype in response to paracrine stimulation, which is regulated by the small Rho-like GTPases (27, 28). The Rho family of small GTPases is a subgroup of Ras superfamily of GTP-binding proteins. Earlier it was thought of having ~10 members but now it consists of >100 (29, 30). They are further subdivided into 6 families based on the sequence homology and function, and these families are Ras, Rho, Rab, Arf, Ran, and Rad/Gem. Each family consists of several members with distinct expression, cellular localization, and biological activities (30). Their activation causes specific reorganization(s) of the cells' cytoskeleton. GTPases have been implicated in pleiotropic-signaling events ranging from cell adhesion, spreading, motility, membrane trafficking, transcription activation, cell cycle progression, and cell fate determination (27, 28).

Several Rho family proteins have been implicated in Ras oncogenic transformation, suggesting that they contribute to the aberrant growth properties of transformed cells (31). Overexpression of RhoA, Cdc42, and Rac were reported in colon and lung carcinomas with the most dramatic difference noted in the RhoA level in human breast cancer as compared with the corresponding normal tissues (29–32). Rac1 was found to be overexpressed in human breast cancer together with a mutant form of Rac1 (Rac1b; Ref. 29), and elevated expression of RhoC was observed in a human breast cancer and ductal adenocarcinoma of the pancreas (33, 34). Recently, a DNA array analysis revealed that RhoC has an important role in tumor cell invasion because it enhances the metastasis when overexpressed, whereas dominant-negative Rho inhibits the metastasis (35).

Here, we report on the changes in the morphology, cytoskeleton, and the expression of small GTPases induced by AMF stimulation in the human A375 melanoma cells. In addition, we demonstrate that activation of AMF receptor leads to the formation of stress-fiber-like structures in the melanoma cells in a RhoA-dependent manner.

Received 2/26/02; accepted 6/3/02.

The costs of publication of this article were defrayed in part by the payment of page charges. This article must therefore be hereby marked *advertisement* in accordance with 18 U.S.C. Section 1734 solely to indicate this fact.

<sup>1</sup> Supported by National Cancer Institute Grant R01CA 51714 (to A. R.).

<sup>2</sup> To whom requests for reprints should be addressed, at Metastasis Research Program, Karmanos Cancer Institute, 110 East Warren Avenue, Detroit, MI 48201. Phone: (313) 833-0960; Fax: (313) 831-7518; E-mail: raza@Kci.wayne.edu.

<sup>3</sup> The abbreviations used are: AMF, autocrine motility factor; PHI, phosphohexose/glucose isomerase; NLK, neuroleukin; JNK, c-Jun NH<sub>2</sub>-terminal kinase; PBS-T, PBS plus Tween-20; TRITC, tetramethylrhodamine isothiocyanate; AMV, avian myeloblastosis virus; SAPK, stress-activated protein kinase; RT-PCR, reverse transcription-PCR; MAPK, mitogen-activated protein kinase; HRG, heregulin.

## MATERIALS AND METHODS

**Cell Culture.** Human malignant melanoma A375 (ATCC CRL 1619) cells and human fibrosarcoma HT1080 (ATCC CCL 121) were obtained from American Type Culture Collection (Manassas, VA). Cells were grown in DMEM supplemented with 10% heat-inactivated fetal bovine serum (Summit Biotechnology, Fort Collins, CO) plus essential and nonessential amino acids, penicillin-streptomycin (Life Technologies, Inc., Grand Island, NY). The cultures were maintained in a humidified chamber with 95% air and 5% CO<sub>2</sub> at 37°C. Cells were harvested and passed for experiments with 0.25% trypsin and 0.025% EDTA, and viability was monitored by trypan blue exclusion.

**Antibodies and Reagents.** Monoclonal antibodies directed against Cdc42, Rac1, and RhoA were purchased from Transduction Laboratories (Lexington, KY). The antibodies directed against JNK were purchased from Promega Corporation (Madison, WI). Horseradish peroxidase-conjugated goat antirabbit IgG and antimouse IgG were purchased from Zymed Laboratories (South San Francisco, CA). Recombinant AMF was produced in *Escherichia coli* as described previously (36).

**SDS-PAGE and Western Blotting.** Aliquots of cell lysates from various treatments were used with equal amounts of protein loaded in each lane. All protein samples were separated either on 8 or 12.5% SDS-PAGE separating gels and 3.5% stacking gels with Tris-glycine system and blotted onto a polyvinylidene fluoride membrane (MSI; Westborough, MA). The blots were blocked with 5% nonfat dry milk in PBS containing 0.1% PBS-T either for 1 h at room temperature or overnight at 4°C. The blots were incubated with primary antibody diluted (Cdc42, 1:2500; RhoA, 1:500; Rac1, 1:1,500; and JNK in PBS-T, 1:5,000) and incubated for 1 h, except JNK, which was incubated for 2 h at room temperature. Afterward, these blots were washed in PBS-T three times for 15 min and incubated with either antimouse or antirabbit secondary antibody horseradish peroxidase conjugate. Blots were then treated with enhanced chemiluminescence (Amersham, Arlington Heights, IL) reagent to visualize the bands, and results were obtained on Kodak Bio-Max MR film (Eastman Kodak Company, Rochester, NY). Density of the bands was determined by a Kodak imaging system and equalized by  $\beta$  actin.

**Cell Motility Assay.** Cell motility was measured by a 48-well-modified Boyden-chamber (4, 34). Briefly, 5 mg/ml fibronectin in PBS were placed in a lower chamber, which was separated from the upper chamber by a pore membrane (8  $\mu$ m). A single cell suspension of  $5 \times 10^4$  A375 melanoma cells in serum-free medium containing different concentrations of recombinant AMF was placed in the upper chamber. After 5 h of incubation at 37°C, the cells were fixed in methanol and stained with H&E. The cells that migrated through the pores to the lower surface of the filter were counted under a microscope. A total of 10 random fields was counted from quadruplicate assays.

**Cells' Response to AMF.** To study the effect of AMF on cells, cells were either grown in 100-mm dishes for harvesting or passaging on a coverslip in 6-well plates for morphological and immunofluorescence studies. When cells were ~70–80% confluent, cells were kept on serum-free media for 24 h before the experiment. After 24 h of serum starvation, old media were replaced with new serum-free media containing various concentrations of AMF (0, 1, 10, and 30 ng/ml), and cells were treated for 60 min at 37°C. Then, media were removed; cells were washed with cold PBS and scraped with 1.0 ml of cold PBS. Cells were spun down at 1500 rpm for 5 min at 4°C, and pellet was kept at –70°C for 15 min. Cells were lysed in radioimmunoprecipitation assay lysis buffer [0.02 M Tris-HCl (pH 7.5) + 0.1% SDS + 1.0% Triton-X-100 + 1.0% sodium dextrocholate + mixture of protease inhibitors] and kept on ice for 30 min. Finally, cell lysate was centrifuged at 15,000 rpm at 4°C for 30 min, and the supernatant was saved for additional analysis. The protein content of supernatant samples was measured by the Bio-Rad method (Protein dye reagent; Bio-Rad Laboratories, Hercules, CA).

**Immunofluorescence Staining.** Cells were grown on coverslips ( $1 \times 10^4$  cells) in DMEM containing 10% fetal bovine serum. Cells were kept on serum-free media for 24 h before the experiment. Cells were treated with various concentrations of AMF (0, 1, and 10 ng/ml) for 60 min at 37°C. Actin filaments were visualized in cells fixed in 3.7% paraformaldehyde for 30 min using TRITC-conjugated phalloidin (1:100 dilution in PBS) for 30 min at room temperature.

For antigen, visualization cells were fixed with methanol at –20°C for 10 min. The cells were blocked with 1.0% BSA in PBS for 20 min at room

temperature and then incubated with primary antibody Cdc42 or RhoA (1:100 dilution in 0.1% BSA in PBS) for 4°C for 1 h. After incubation with primary antibody, cells were washed three times with 0.1% BSA in PBS. Cells were incubated with FITC-conjugated secondary antibody antimouse IgG (1:200 dilution in 0.1% BSA in PBS) for 4°C for 1 h, followed by three washes with 0.1% BSA in PBS and one washing with PBS. Coverslips were then mounted on a glass slide with a drop of SlowFade reagent (Molecular Probes, Eugene, OR).

**Assay of Active-Cdc42, -RhoA, and -Rac1 Activities.** Activation status of Cdc42, RhoA, and Rac1 was assayed using fusion protein GST-PAK-CRIB domain (37, 38) and GST-21 as described (39). A375 cell lysates from treated and control cultures were analyzed for bound Cdc42, Rac1, and RhoA molecules by Western blot analysis using specific antibody for each protein as described in Western blot analysis.

**Analysis of the Expression of RhoA, Rac1, and Cdc42 by RT-PCR.** Confluent A375 cell monolayers were serum starved for 24 h and exposed to 30.0 ng/ml AMF in serum-free media. RNA was isolated using TRIzol reagent according to the manufacturer's instructions (Life Technologies, Inc., Gaithersburg, MD). The quality of RNA was checked by 260:280 ratio and running a 1.0% RNA gel. RT-PCR was performed using Access RT-PCR system of Promega (Promega Corporation). Briefly, the reaction mixture consists of 1 mg total RNA, AMV/Tfi 5X reaction buffer, deoxynucleotide triphosphate mix, specific upstream and downstream primers, and 25 mM MgSO<sub>4</sub> in thin-walled 0.5-ml reaction tubes. To these were added AMV reverse transcriptase and Tfi DNA polymerase. The tubes were incubated at 48°C for 45 min. Immediately after the tubes were transferred to a thermocycler (GeneMate; ISC BioMax, Kavsville, UT), they were subjected to the following cycles: 1 cycle at 94°C for 2 min for AMV reverse transcriptase inactivation and RNA/cDNA/primer denaturation; 40 cycles consist of 94°C for 30 s denaturation, 60°C for 1 min annealing, and 68°C for 2 min extension; 1 cycle 68°C for 7 min final extension; and 1 cycle at 4°C to soak.

Finally, the PCR product was separated on 3% NuSieve/1% agarose along with 100-bp Ladder (Promega Corporation).

The following primers were used: RhoA Upstream CTGGTGATTGTG-GTGATGG size 183 bp (31) and Downstream GCGATCATAATCTTCTCCT-GCC; B2m Upstream ACCCCCACTGAAAAAGATGA size 203 bp (31) and Downstream ATCTTCAAACCTCCATGATG; Rac1 Upstream ATGCAG-GCCATCAAGTGTGTGGTG size 600 bp (27) and Downstream TTACAA-CAGCAGGCATTTTCTCTTCC; Cdc42 Upstream TCTCCTGAATGATG-GTCTGGG size 250 bp and Downstream GATAGAGTGGAAAAGGGA GTAGG.

**Treatment of Cells with Exoenzyme C3.** Exoenzyme C3 was purchased from Calbiochem (San Diego, CA) and was introduced into A375 cells with lipofectAmine (Life Technologies, Inc.). Exoenzyme C3 (3.5 mg/35 mm dish) was mixed with 100  $\mu$ l of serum-free DMEM. In another tube, 25  $\mu$ l of lipofectAmine reagent were mixed with 100  $\mu$ l of serum-free DMEM. Both solutions were mixed gently by drop-wise addition and incubated for 45 min at room temperature. After incubation, 800  $\mu$ l of additional serum-free medium were added and solutions gently mixed and overlaid on the cells. Cells were incubated at 37°C for 5 h. The control cells received same treatment, except that exoenzyme C3 was omitted.

**Statistical Analysis.** Significant values were determined using two-tailed nonparametric Tukey's test using the StatMost program. The results are expressed as mean values  $\pm$  SE.  $P < 0.05$  was considered as significant.

## RESULTS

**An AMF-dependent Cytoskeletal and Morphological Change in A375 and HT1080 Cells.** A375 melanoma cells secrete and respond to AMF in an autocrine fashion with increased cell motility (36). Here, we first question whether A375 human melanoma cells would respond to a recombinant human AMF that will allow investigation of its signaling pathway. As shown in Fig. 1, recombinant AMF effectively stimulates A375 melanoma cell motility, verifying that the recombinant human AMF is properly folded and biologically active. To determine whether actin plays a role in AMF-induced cell migration, we examined the pattern and morphology of the actin filaments. It can be seen from Fig. 2 that AMF stimulation leads to the reorga-

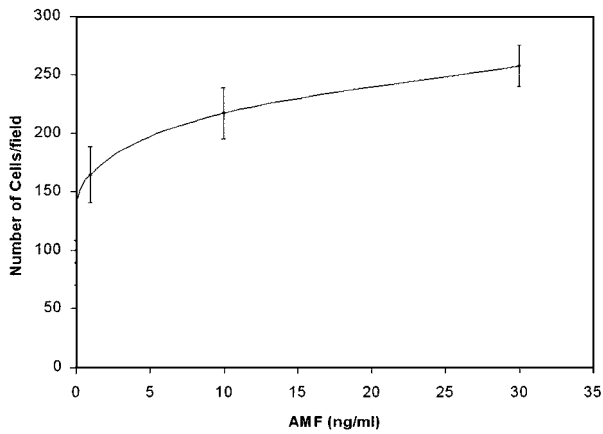


Fig. 1. Dosage-dependent cell motility-stimulating activity of purified recombinant human AMF. Human melanoma A375 cell motility was analyzed by Boyden-chamber assay. Bars, SE of quadruple analyses.

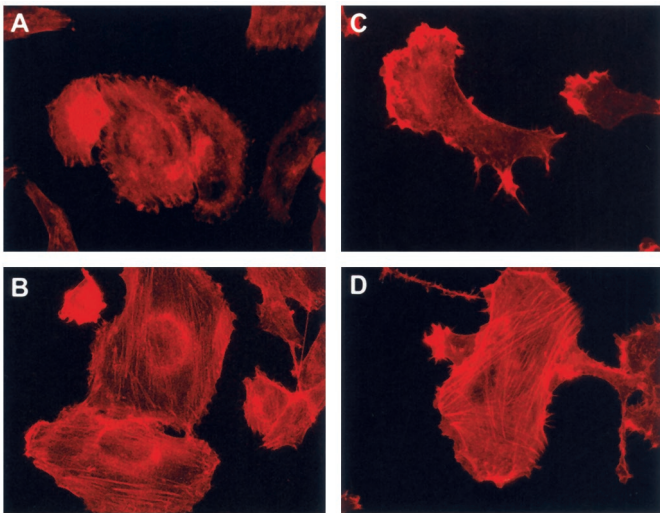


Fig. 2. Immunofluorescence detection of actin organization in A375 melanoma and HT1080 fibrosarcoma cells. Twenty-four-h serum-starved cells were incubated with 30 ng/ml recombinant AMF for 60 min. Cells were then washed, fixed, and stained with TRITC-phalloidin. A and B, A375 cells (control) and AMF-treated cells, respectively. C and D, A375 cells HT1080 cells (control) and AMF-treated cells, respectively.

nization of the actin molecules leading to the formation of heavy bundles of stress-fiber-like structures transversing the cells (Fig. 2, A and B). This observed effect of AMF is not unique to the A375 melanoma-responding cells as similar cytoskeletal rearrangement was induced by AMF in a different cell line of a different histopathological origin, *i.e.*, HT1080 fibrosarcoma (Fig. 2, C and D).

**Immune Localization of RhoA and Cdc42 in A375 Melanoma and HT1080 Fibrosarcoma Cells.** To determine the response of small GTPases in AMF-induced motility and cytoskeletal rearrangement in cells, we studied their expression and subcellular distribution after AMF stimulation. Cells were serum starved for 24 h and then incubated with (30.0 ng/ml) or without AMF for 60 min at 37°C. After washing, the cells were fixed and immunostained for the localization of RhoA (Fig. 3) and Cdc42 (Fig. 4).

The comparison of the cellular distribution pattern of RhoA in the untreated cells (Fig. 3, A and C) *versus* AMF-treated A375 and HT1080 cells (Fig. 3, B and D), respectively, revealed that AMF induced redistribution of RhoA from a uniform cellular distribution to the lamellipodia and filopodia at the leading edges of the cells' periphery, whereas the cellular localization of Cdc42 was refractory to

AMF (Fig. 4). Cdc42 was uniformly distributed throughout the cytoplasm of both A375 (Fig. 4, A and B) and HT1080 cells (Fig. 4, C and D) in the control (Fig. 4, A and C) and the AMF-treated cells (Fig. 4, B and D).

**AMF-dependent Rac1 Expression.** To gain additional insight into the signaling events of AMF manifested by the above structural changes, we next analyzed the level of Cdc42, Rac1, and RhoA GTPases proteins in AMF-stimulated *versus* -resting A375 melanoma cells. We assayed for levels of both active Rac1 and total Rac1 using GST-PAK-CD that specifically binds to active Rac1 (Fig. 5A; Refs. 37, 38). Treatment with AMF induced a marked elevation in the level of active Rac1 (Fig. 5A) in a dosage-dependent manner. By densitometric-tracing analysis, we have determined that the level of active Rac1 has increased by a 2.6-fold, whereas the expression level of total

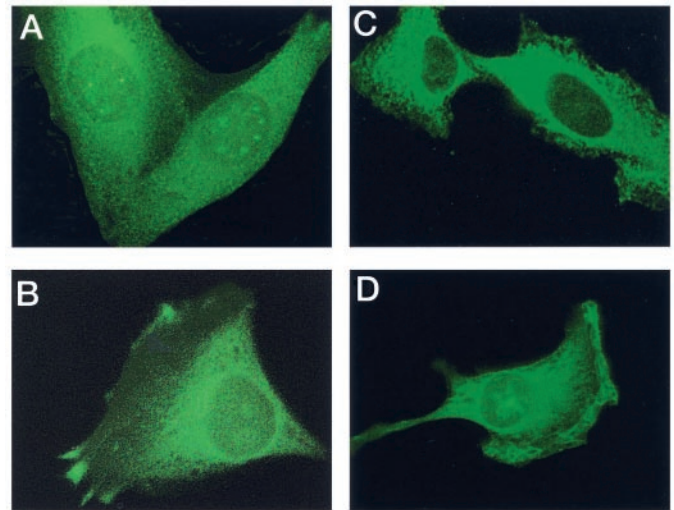


Fig. 3. Immunofluorescence localization of RhoA in A375 melanoma and HT1080 fibrosarcoma cells. Twenty-four-h serum-starved cells were incubated with 30.0 ng/ml of AMF for 60 min. Cells were then washed, fixed, and incubated with anti-RhoA specific antibodies, followed by incubation with FITC-conjugated antimouse secondary antibody. A and B, A375 cells (control) and AMF-treated cells, respectively. C and D, HT1080 cells (control) and AMF-treated cells, respectively.

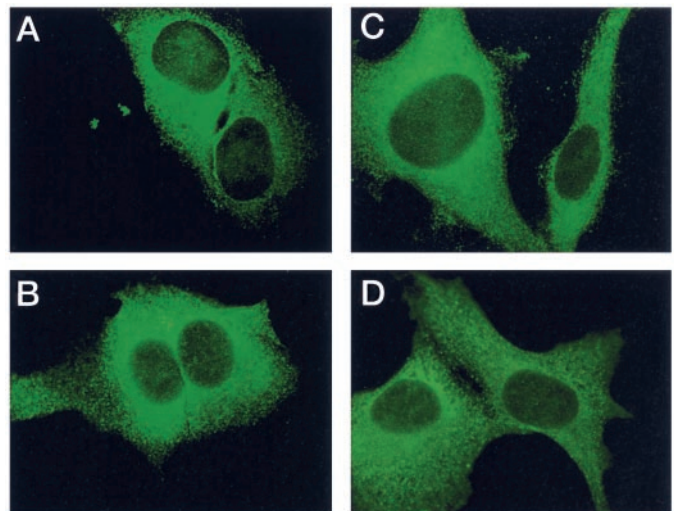


Fig. 4. Immunofluorescence localization of Cdc42 in A375 melanoma and HT1080 fibrosarcoma cells. Twenty-four-h serum-starved cells were incubated with 30.0 ng/ml of AMF for 60 min. Cells were then washed, fixed, and incubated with anti-Cdc42 specific antibodies, followed by incubation with FITC-conjugated secondary antibody. A and B, A375 cells (control) and AMF-treated cells, respectively. C and D, HT1080 cells (control) and AMF-treated cells, respectively.

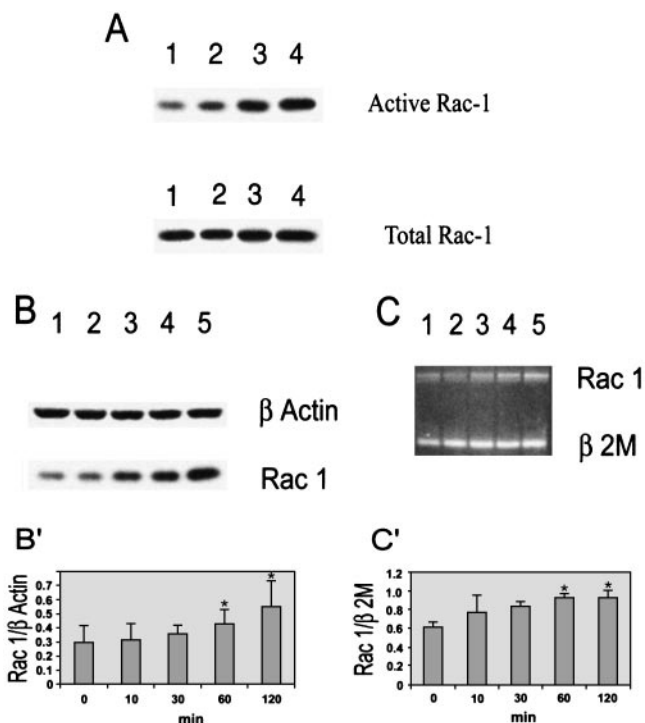


Fig. 5. Basal and activation status of A375 melanoma cells' Rac in response to AMF. A375 cells' lysates were prepared after treatments with various concentrations of AMF (0–30.0 ng/ml AMF) were analyzed for the levels of Rac-1. *A*, active Rac1 protein was pulled down by GST-fusion protein (GST-PAK-CD), separated on SDS-PAGE, and detected by Western blot analysis 1 (control), 2 (1.0 ng/ml), 3 (10.0 ng/ml), and 4 (30.0 ng/ml) AMF, respectively. *B*, time-dependent changes in the expression of Rac1 by stimulation with AMF. Cells were treated with 30 ng/ml AMF for various time points: *Lane 1*, 0 min; *Lane 2*, 10 min; *Lane 3*, 30 min; *Lane 4*, 60 min; and *Lane 5*, 120 min. *B'*, densitometric analysis of the result in *B*. \* denotes significant difference compared with control, ( $P < 0.05$ ). *C*, time-dependent changes in expression levels of Rac1 mRNA. Cells were treated with 30 ng/ml of AMF for various time points: *Lane 1*, control; *Lane 2*, 10 min; *Lane 3*, 30 min; *Lane 4*, 60 min; and *Lane 5*, 120 min. At the end, total RNA was isolated and was used to measure the expression of Rac1 using RT-PCR. *C'*, densitometric tracing analysis of the result shown in *C*. \* denotes significant difference compared with control ( $P < 0.05$ ). Bars, SE of triplicate analyses.

Rac1 has increased slightly by only 1.8-fold in cells stimulated with AMF as compared with control-resting cells, respectively. The time-dependent changes in the cellular level of Rac1 protein and mRNA expression induced by AMF are shown in Fig. 5, *B* and *B'* and Fig. 5, *C* and *C'*, respectively. The response to AMF is rapid; within 30 min both Rac1 protein and mRNA levels were elevated, the effect persisted up to 120 min. This up-regulation in the expression level of Rac1 is highly reproducible, significant, and appears to be sufficient to transduce motile signaling.

Next, the levels of active and total cellular RhoA were determined by using GST-C21 fusion protein consisting of Rho downstream effector Rhotekin (39). The results presented in Fig. 6A reveal that AMF signaling leads to an activation of RhoA (Fig. 6A). A densitometric-tracing analysis revealed that active RhoA protein level was increased by 2.18 in response to AMF as compared with resting cells, respectively. To investigate whether the cellular level of Cdc42 will be similarly changed, we tested the expression levels of active and total Cdc42 (Fig. 7A) and mRNA (Fig. 7B). These activations of Rac1 and RhoA by AMF were blocked by anti-AMF antibody (data not shown). Stimulation of A375 cells by AMF resulted in no significant alteration in the level of either active Cdc42 (Fig. 7A, top panel) or total Cdc42 (Fig. 7A, bottom panel). Time-dependent analysis in the expression level of Cdc42 protein (data not shown) or mRNA (Fig. 7B) reiterated that Cdc42 was refractory to AMF stimulation and supports the data shown in Fig. 4. These results are reminiscent to

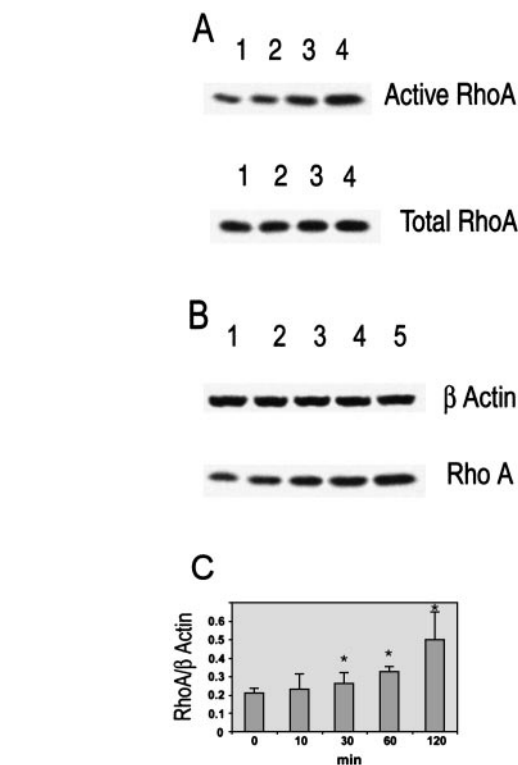


Fig. 6. Basal and activation status of A375 melanoma cells' RhoA in response to AMF. *A*, A375 cell lysates were prepared after treatment with various concentrations of AMF (0–30.0 ng/ml). Active RhoA protein was pulled down by incubating cell lysates with GST-fusion protein (GST-C21), separated on SDS-PAGE, and detected by Western blot analyses. Aliquots of respective cell lysate were also used to analyze the total RhoA using Western analysis: *Lane 1*, control; *Lane 2*, 1.0 ng/ml; *Lane 3*, 10.0 ng/ml; and *Lane 4*, 30.0 ng/ml AMF, respectively. *B*, time-dependent changes in the expression of RhoA upon AMF stimulation. Cells were treated with 30 ng/ml AMF for various time points, 0–120 min. Cell lysates were used to analyze the expression of RhoA using Western blot analysis: *Lane 1*, control; *Lane 2*, 10 min; *Lane 3*, 30 min; *Lane 4*, 60 min; and *Lane 5*, 120 min, respectively, after AMF treatment. *C*, densitometric tracing analysis of the results presented in *B*. \* denotes significant difference compared with control ( $P < 0.05$ ).

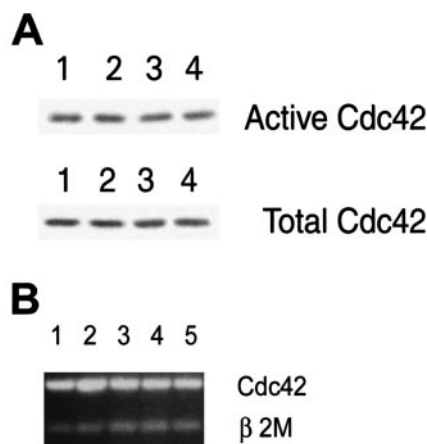


Fig. 7. Basal and activation status of A375 melanoma cells Cdc42 in response to AMF. *A*, A375 cell lysates were prepared after treatment with various concentrations (0–30 ng/ml) of AMF. Active Cdc42 protein was pulled down by incubating cell lysates with GST-fusion protein (GST-PAK-CD), separated on SDS-PAGE, and detected by Western blot analyses. Aliquots of respective cell lysates were used to analyze the total Cdc42 by Western analyses: *Lane 1*, control; *Lane 2*, 1.0 ng/ml; *Lane 3*, 10.0 ng/ml; and *Lane 4*, 30.0 ng/ml AMF, respectively. *B*, time-dependent study on the expression level of Cdc42 mRNA by RT-PCR. Cells were treated with 30 ng/ml AMF for various time points: *Lane 1*, control; *Lane 2*, 10 min; *Lane 3*, 30 min; *Lane 4*, 60 min; and *Lane 5*, 120 min. The data shown is representative of three independent experiments with similar results.

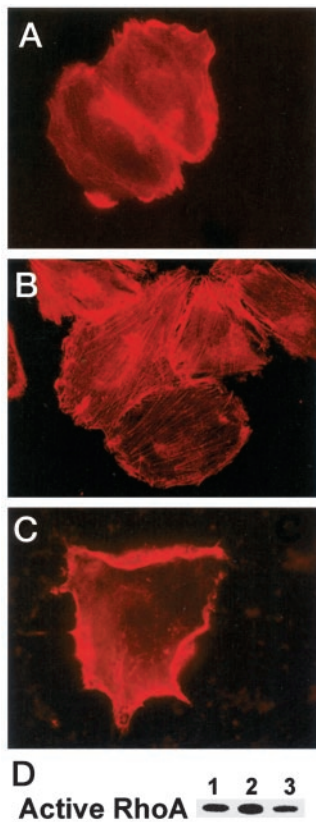


Fig. 8. C3 exoenzyme inhibits AMF-induced actin organization. A375 cells were treated with 3.5 mg/ml C3 exoenzyme using the lipofectAmine technique, whereas control cells were treated with lipofectAmine alone. Twenty-four-h serum-starved A375 melanoma cells were kept in serum-free media for 24 h before the experiment and then treated with 30.0 ng/ml AMF for 60 min at 37°C. *A*, control; *B*, AMF; and *C*, AMF and C3 exoenzyme. Washing, fixation, and staining with TRITC phalloidin-terminated experiments. *D*, Western blot analysis of active RhoA in A375P cells pretreated with C3 exoenzyme before the treatment of AMF. Parallel cell cultures to the above were lysed and active RhoA protein was pulled down by incubating the cell lysate with GST-fusion protein (GST-C21). The cell extracts were separated on SDS-PAGE and detected by Western blot analyses: Lane 1, control; Lane 2, AMF; and Lane 3, AMF and C3 exoenzyme. The data shown is a representative of two independent experiments showing similar results.

those showing that platelet-derived growth factor stimulation of NIH-3T3 activates Rac and not Cdc42 (40).

**C3 Exoenzyme Inhibits Stress-Fiber Formation in A375 Melanoma Cells.** In fibroblasts, Rho is required for both the formation and maintenance of actin stress fibers (40, 41). To determine whether similar events occur in melanoma, we analyzed the cytoskeletal changes induced by AMF in the presence of C3 exoenzyme, a specific inhibitor of Rho. As depicted in Fig. 7, A375 cells respond to AMF by rearranging the actin fibers into the formation of the stress-fiber structure traversing the cells (Fig. 8*B*), whereas C3 exoenzyme inhibited stress-fiber formation (Fig. 8*C*), indicating that AMF-induced stress fiber formation is dependent on Rho activity. To further establish that RhoA responds to AMF, the expression of active RhoA was studied in serum-starved A375 melanoma cells pretreated with C3 exoenzyme before AMF stimulation. In agreement with the above, a link between AMF-mediated receptor stimulation and RhoA activation was observed. AMF-induced a 2.4-fold increase in the level of active RhoA (Fig. 8*B*, Lane 2) over the control (Fig. 8*B*, Lane 1), whereas C3 exoenzyme inhibited this up-regulation of active RhoA expression level (Fig. 8*C*, Lane 3). Moreover, A375 cells motility induced by AMF was inhibited by C3 exoenzyme (data not shown).

To further study how these small GTPases are functioning in response to AMF signaling, we followed the expression of active

JNK, also known as SAPK, in A375 melanoma cells. The results show that stimulation of cells with AMF results in the increased expression of both JNK1 and JNK2 isoforms in a dosage-dependent manner (Fig. 9*A*). At the highest AMF concentration used (30 ng/ml), the expression of JNK1 and JNK2 was significantly elevated and reached saturation (Fig. 9*B*). The increased levels for both active JNK1 and JNK2 were 2.07- and 1.67-fold, respectively, consistent with the observed Rac activation (Fig. 5).

## DISCUSSION

One characteristic and probably the most devastating aspect of malignant tumors is their ability to metastasize, a process which involves tumor cell migration from the primary site of growth to distant organs. However, it is still debatable how this necessary attribute, inherent to properly functioning cells of the body, is mis-guided by tumor cells into such a sinister role in the progression of cancer. At different times during tumor cell migration/invasion, they respond to various motile-inducing soluble and insoluble factors in the extracellular milieu. These factors fall into broad categories: paracrine and autocrine mediators. Paracrine factors are generally produced by stromal cells, a prototypical paracrine molecule of this class is the Scatter Factor. The Scatter Factor plays a role in epithelial tumor cell invasion and metastasis as it leads to increased cell motility associated with cytoskeletal rearrangement and signaling through small GTPases (42, 43). Autocrine factors, by their very nature, act upon the cells that secrete them. Notable among them are migratory-stimulating factor, the glioma-produced motility factor, the invasion-stimulating factor, autotaxin, and AMF (for review see Ref. 44). Their functions should be unveiled, in part, through identification of the signaling pathway(s) mediated by their receptor activation. AMF signaling is initiated by its binding to a cell surface 78 kDa seven transmembrane glycoprotein and inhibited by *Bordetella pertussis* toxin, which irreversibly blocks the activity of G proteins (24).

During the last decade, significant attention has been focused on the family of small Rho-like GTPases and their functional role in transducing motility signaling. The signal transduction pathways regulated by Cdc42, Rac1, and RhoA modulate distinct cytoskeletal rearrangement necessary for cell motility (28). The formation of cytoskeletal structure such as lamellipodia, filopodia, and stress fibers often is associated with cell migration, and it appears that Rac produces the

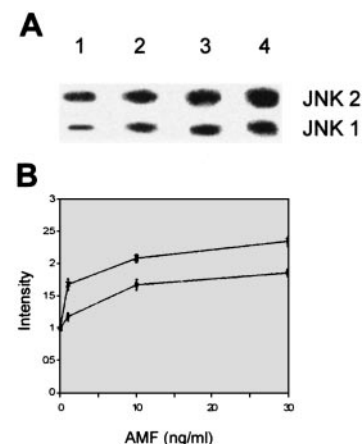


Fig. 9. JNK expressions in AMF stimulated A375 melanoma cells. Cell lysates were prepared from A375 cells after treatment with various concentrations of AMF (0–30.0 ng/ml) for 60 min. *A*, Western blot analyses of the levels of active JNK1 and JNK2: Lane 1, control; Lane 2, 1.0 ng/ml; Lane 3, 10.0 ng/ml; and Lane 4, 30.0 ng/ml AMF, respectively. *B*, densitometric tracing analysis of the results presented in *A*. JNK1 (□) and JNK2 (×).

protrusive activity necessary to drive movement. On the other hand, Cdc42 does not have a major role in the migratory process *per se* but establishes cell polarity to ensure that migration occurs in a specific direction (40, 45). Rac1 and Cdc42 may cooperate to promote spatially defined protrusive activity, whereas the role of the RhoA appears to be more complicated.

Here, we show that AMF activates small GTPases in human melanoma cells. AMF increases stress-fiber formation in a time- and a dosage-dependent manner in cells concomitantly with activation of RhoA and Rac1 with no apparent change in Cdc42. The casual relationship between AMF stimulation and RhoA activation was supported by the observation that the treatment of the cells with C3 exoenzyme, before AMF stimulation, inhibited the formation of stress-fiber-like structures, and the cells did not respond by stimulation of expression of RhoA. In addition, the two isoforms of JNK (JNK1 and JNK2) were concomitantly activated by AMF, suggesting that both may be involved in the signaling pathway of RhoA. These results are consistent with an earlier report showing that AMF induced extensive and rapid cytoskeletal rearrangement in mouse melanoma cells (46), whereby the cells responded to AMF by the formation of stress fibers and accumulation of cortical actin, followed by remodeling of phosphotyrosine plus adhesion plaques to the poles of the stress fibers and translocation of protein kinase C  $\alpha$  to stress fibers and to cortical actin (46).

Here, we questioned whether the small GTPases are part of the AMF signal transduction pathway in A375 melanoma cells. We found that AMF-induced stress-fiber formation was associated with redistribution of RhoA to the leading edges of AMF-stimulated cells and with a significant activation of both Rac1 and RhoA. The apparent observed dichotomy in the cellular response to AMF among Rac1, RhoA, and Cdc42 is supported by earlier findings showing that bradykinin stimulates the expression of Cdc42, whereas platelet-derived growth factor, insulin, and bombesin stimulate the expression of Rac1 (for review see Ref. 47), and lipopoly saccharides and bombesin directly stimulate the expression RhoA (48).

Next, we have examined the levels of expression of JNKs in response to AMF motile stimulation of A375 melanoma cells. Previously, it has been reported that the JNK/SAPK and p38 MAPK cascades are involved in the regulation of gene transcription in response to cellular stress such as UV light, osmotic shock, or inflammatory stimuli (49). Also, it has been reported that overexpression of activated Rac and Cdc42 leads to the activation of the JNK and p38<sup>MAPK</sup> kinase pathways in a variety of cell types (50, 51), and activation of JNK by growth factors and cytokines (epidermal growth factor and tumor necrosis factor  $\alpha$ ) can be inhibited by dominant-negative Rac and Cdc42 (52, 53). The results presented here suggest that in melanoma cells' response to AMF, Rac1 and RhoA activate the JNK/SAPK cascade similarly to the effects of transforming growth factor  $\beta$ -mediated signaling on the epithelium (53). Furthermore, in human breast carcinoma cells, HRG  $\beta$ 1, a combinatory ligand for human epidermal growth factor receptors 3 and 4, stimulates cell motility while it significantly up-regulates the expression of AMF (54). In addition, specific inhibitors of p24/44 MAPK and p38 MAPK, while anti-AMF antibodies suppressed HRG-induced cell scattering (54), inhibited the HRG-induced stimulation of AMF expression.

In this study, we show that AMF is an activator of Rho and Rac1 and promotes rapid cytoskeletal rearrangement associated with induction of cell motility. The data presented here provide an insight into the AMF-signaling pathway and based on the reports of others, we may conclude that this signaling is in many molecular respects similar to the well-characterized paracrine motile-signaling pathway involving Rho and Rac through cytoskeleton rearrangement and JNK/SAPK cascade.

## REFERENCES

1. Trinkaus, J. P. *Cells into Organs: The Forces That Shape of the Embryo*. Englewood Cliffs, NJ: Prentice-Hall, 1984.
2. Boguski, M. S., and McCormick, F. Proteins regulating Ras and its relatives. *Nature (Lond.)*, **366**: 643–654, 1993.
3. Genda, T., Sakamoto, M., Ichida, T., Asakura, H., Kojiro, M., Narumiya, S., and Hirohashi, S. Cell motility mediated by Rho and Rho-associated protein kinase plays a critical role in intrahepatic metastasis of human hepatocellular carcinoma. *Hepatology*, **30**: 1027–1036, 1999.
4. Liotta, L. A., Mandler, R., Murano, G., Katz, D. A., Gordon, R. K., Chiang, P. K., and Schiffmann, E. Tumor cell autocrine motility factor. *Proc. Natl. Acad. Sci. USA*, **83**: 3302–3306, 1986.
5. Silletti, S., Watanabe, H., Hogan, V., Nabi, I. R., and Raz, A. Purification of B16–F1 melanoma autocrine motility factor and its receptor. *Cancer Res.*, **51**: 409–414, 1991.
6. Watanabe, H., Carmi, P., Hogan, V., Raz, T., Silletti, S., Nabi, I. R., and Raz, A. Purification of human tumor cell autocrine motility factor and molecular cloning of its receptor. *J. Biol. Chem.*, **266**: 13442–13448, 1991.
7. Watanabe, H., Takehana, K., Date, M., Shinozaki, T., and Raz, A. Tumor cell motility factor is neuroleukin/phosphohexose isomerase polypeptide. *Cancer Res.*, **56**: 2960–2963, 1996.
8. Chaput, M., Claes, V., Portetelle, D., Cludts, I., Cravador, A., Burny, A., Gras, H., and Tartar, H. The neurotrophic factor neuroleukin is 90% homologous with phosphohexose isomerase. *Nature (Lond.)*, **332**: 454–455, 1988.
9. Gurney, M. E., Heinrich, S. P., Lee, M. R., and Yin, S.-H. Molecular cloning and expression of neuroleukin, a neurotrophic factor for spinal and sensory neurons. *Science (Wash. DC)*, **234**: 566–574, 1986.
10. Niinaka, Y., Paku, S., Haga, H., Watanabe, H., and Raz, A. Expression and secretion of neuroleukin/phosphohexose isomerase/maturation factor as autocrine motility factor by tumor cells. *Cancer Res.*, **58**: 2667–2674, 1998.
11. Xu, W., Seither, K., Feldman, E., Ahmed, T., and Chiao, J. W. The differentiation and maturation mediator for human myeloid leukemia cells shares homology with neuroleukin or phosphoglucose isomerase. *Blood*, **87**: 4502–4506, 1996.
12. Chiao, J. W., Xu, W., Seither, K., Feldman, E., and Ahmed, T. Neuroleukin mediated differentiation induction of myelogenous leukemia cells. *Leuk. Res.*, **23**: 13–18, 1999.
13. Cao, M. J., Osatomi, K., Matsuda, R., Ohkuba, M., Hara, K., and Ishihara, T. Purification of a novel serine proteinase inhibitor from the skeletal muscle of white croaker (*Argyrosomus argentatus*). *Biochem. Biophys. Res. Commun.*, **272**: 485–490, 2000.
14. Harrison, R. A. P. The detection of hexosekinase, glucosephosphate isomerase, and phosphoglucose isomerase activities in polyacrylamide gel after electrophoresis: a novel method using immobilized glucose 6-phosphate dehydrogenase. *Anal. Biochem.*, **61**: 500–507, 1974.
15. Baumann, M., and Brand, K. Purification and characterization of phosphohexose isomerase from human gastrointestinal carcinoma and its potential relationship to neuroleukin. *Cancer Res.*, **48**: 7018–7021, 1988.
16. Baumann, M., Kappel, A., Brand, K., Siegfried, W., and Paterson, K. The diagnostic validity of the serum tumor marker phosphohexose isomerase (PHI) in patients with gastrointestinal, kidney, and breast cancer. *Cancer Investig.*, **8**: 351–356, 1990.
17. Filella, X., Molina, R., Jo, J., Mas, E., and Ballesta, A. M. Serum phosphohexose isomerase activities in patients with colorectal cancer. *Tumor Biol.*, **12**: 360–367, 1991.
18. Patel, P. S., Rawal, G. N., Rawal, R. M., Patel, G. H., Balar, D. B., Shah, P. M., and Patel, D. D. Comparison between serum levels of carcinoembryonic antigen, sialic acid, and phosphohexose isomerase in lung cancer. *Neoplasma (Bratisl.)*, **42**: 271–274, 1995.
19. Bodansky, O. Serum phosphohexose isomerase in cancer. II. As an index of tumor growth in metastatic carcinoma of the breast. *Cancer (Phila.)*, **7**: 1200–1226, 1954.
20. Schwarz, M. K. Laboratory aids to diagnosis: enzymes. *Cancer (Phila.)*, **37**: 542–548, 1976.
21. Osthus, R. C., Shim, H., Kim, Li, Q., Reddy, R., Mukherjee, M., Xu, Y., Wonsley, D., Lee, L. A., and Dang, C. V. Deregulation of glucose transporter 1 and glycolytic gene expression by c-Myc. *J. Biol. Chem.*, **275**: 21797–21800, 2000.
22. Matsumoro, I., Staub, A., Benoist, C., and Mathis, D. Arthritis provoked by a linked T and B cell recognition of a glycolytic enzyme. *Science (Wash. DC)*, **286**: 1732–1735, 1999.
23. Schaller, M., Burton, D. R., and Ditzel, H. J. Autoantibodies to GPI in rheumatoid arthritis: linkage between an animal model and human disease. *Nat. Immunol.*, **2**: 746–753, 2001.
24. Stracke, M. L., Guirguis, R., Liotta, L. A., and Schiffmann, E. Pertussis toxin inhibits stimulated motility independently of the adenylate cyclase pathway in human melanoma cells. *Biochem. Biophys. Res. Commun.*, **146**: 339–345, 1987.
25. Kohn, E. C., Liotta, L. A., and Schiffmann, E. Autocrine motility factor stimulates three-fold increase in inositol phosphate in human melanoma cells. *Biochem. Biophys. Res. Commun.*, **166**: 757–764, 1990.
26. Silletti, S., Timar, J., Honn, K. V., and Raz, A. Autocrine motility factor induces differential 12-lipoxygenase expression and activity in high- and low-metastatic K1735 melanoma cell variants. *Cancer Res.*, **54**: 5752–5756, 1994.
27. Ridley, A. J., Paterson, H. F., Johnston, C. L., Diekmann, D., and Hall, A. The small GTP-binding protein rac regulates growth factor-induced membrane ruffling. *Cell*, **70**: 401–410, 1992.
28. Hall, A. GTPase and actin cytoskeleton. *Science (Wash. DC)*, **279**: 509–514, 1998.
29. Schmelzer, A., Prechtel, D., Knaus, U., Dehne, K., Gerhard, M., Graeff, H., Harbeck, N., Schmitt, M., and Lengyel, E. Rac1 in human breast cancer: overexpression mutation, analysis, and characteristic of new isoform, Rac1b. *Oncogene*, **19**: 3013–3020, 2000.

30. Aznar, S., and Lacal, J. C. Rho signals to cell growth and apoptosis. *Cancer Lett.*, *165*: 1–10, 2001.
31. Zohn, I. M., Campbell, S. L., Khosravi-Far, R., Rossman, K. L., and Der, C. J. Rho family proteins and Ras transformation: the RHOad less traveled gets congested. *Oncogene*, *17*: 1415–1438, 1998.
32. Fritz, G., Just, I., and Kaina, B. Rho GTPase are over-expressed in human tumors. *Int. J. Cancer*, *81*: 682–687, 1999.
33. Suwa, H., Ohshio, G., Imamura, T., Watanabe G., Arii, S., Imamura, M., Narumiya, S., and Fukumoto, M. Overexpression of the RhoC gene correlates with progression of ductal adenocarcinoma of the pancreas. *Br. J. Cancer.*, *77*: 147–152, 1998.
34. van Golen, K. L., Davies, S., Wu, Z. F., Wang, Y., Bucana, C. D., Root, H., Chandrasekharappa, S., Strawderman, M., Ethier, S. P., and Merajver, S. D. A novel putative low affinity insulin-like growth factor-binding protein. LIBS (lost inflammatory breast cancer) and RhoC GTPase correlates with the inflammatory breast cancer phenotypes. *Clin. Cancer Res.*, *5*: 2511–2519, 1999.
35. Clark, E. A., Golub T. R., Lander, E. S., and Hynes, R. O. Genomic analysis of metastasis reveals an essential for RhoC. *Nature (Lond.)*, *406*: 532–535, 2000.
36. Haga, A., Niinaka, Y., and Raz, A. Phosphohexose isomerase/autocrine motility factor/neuroleukin/maturation factor is a multifunctional phosphoprotein. *Biochim. Biophys. Acta*, *1480*: 235–244, 2000.
37. Sander, E. E., ten Klooster, J. P., van Delft, S., van der Kammen, R. A., and Collard, J. G. Matrix-dependent Tiam1/Rac signaling in epithelial cells promotes either cell-cell adhesion or cell migration and is regulated by phosphatidylinositol 3-kinase. *J. Cell Biol.*, *147*: 1385–1398, 1999.
38. Sander, E. E., ten Klooster, van Delft, S., van der Kammen, R. A., and Collard, J. G. Rac down-regulates Rho activity: reciprocal balance between both GTPases determines cellular morphology, and migratory behavior. *J. Cell Biol.*, *147*: 1009–1021, 1999.
39. Reid, T., Furuyashiki, T., Ishizaki, T., Watanabe, G., Watanabe, N., Fujisawa, K., Morii, N., Madaule, P., and Narumiya, S. Rhotekin, a new putative target for Rho-bearing homology to a serine/threonine kinase, PKN, and rho-philin in the rho-binding domain. *J. Biol. Chem.*, *271*: 13556–13560, 1996.
40. Nobes, D., and Hall, A. Rho, Rac, and cdc42 GTPases regulate the assembly of the multimolecular focal complexes associated with actin stress fibers, lamellipodia, and filopodia. *Cell*, *81*: 53–62, 1995.
41. Ridley, H., and Hall, A. The small GTP-binding protein Rho regulating the assembly of focal adhesion and actin stress fibers in response to growth factor. *Cell*, *70*: 389–399, 1992.
42. Birchmeier, C., and Gherardi, E. Developmental roles HSF/SF and its receptor, the c-met-tyrosine kinase. *Trends Cell Biol.*, *8*: 404–410, 1998.
43. Sakkab, D., Lewitzky, M., Posrn, G., Schaeper, U., Sachs, M., Birchmeier, W., and Feller, S. M. Signaling of hepatocyte growth factor/scatter factor (HGF) to the small GTPase Rap 1 via the large ducking protein Gab1 and adapter protein CRKL. *J. Biol. Chem.*, *275*: 10772–10778, 2000.
44. Silletti, S., Paku, S., and Raz, A. Tumor cell motility and metastasis. *Pathol. Oncol. Res.*, *3*: 230–245, 1997.
45. Allen, W. E., Zicha, D., Ridley, A. J., and Jones, G. E. A role for Cdc42 in macrophage chemotaxis. *J. Cell Biol.*, *141*: 1147–1157, 1998.
46. Timar, J., Toth, S., Tovari, J., Paku, S., and Raz, A. Autocrine motility factor (neuroleukin, phosphohexose isomerase) induces cell movement through 12-lipoxygenase dependent tyrosine phosphorylation and serine dephosphorylation events. *Clin. Exp. Metastasis*, *17*: 809–816, 1999.
47. Aspenstrom, P. The Rho GTPase have multiple effects on the actin cytoskeleton. *Exp. Cell Res.*, *246*: 20–25, 1999.
48. Van Aelst, L., and D'Souza-Schorey, C. Rho GTPase and signaling networks. *Genes Dev.*, *11*: 2295–2322, 1997.
49. Treisman, R. Regulation of transcription by MAP kinase cascades. *Curr. Opin. Cell Biol.*, *8*: 205–215, 1996.
50. Minden, A., Lin, A., Claret, F. X., Abo, A., and Karin, M. Selective activation of the JNK signaling cascade and c-Jun transcriptional activity by small GTPases Rac and CDC42HS. *Cell*, *81*: 1147–1157, 1995.
51. Bagrodia, S., Derijard, B., Davis, R. J., and Cerione, R. A. Cdc42 and PAK-mediated signaling leads to Jun kinase and p38 mitogen-activated protein kinase activation. *J. Biol. Chem.*, *270*: 27995–27998, 1995.
52. Cosco, O. A., Chiariello, M., Yu, J. C., Termoto, H., Crespo, P., Xu, N., Milkim, T., and Gutkind, J. S. The small GTP-binding protein Rac1 and cdc42 regulates the activity of the JNK/SAPK signaling pathway. *Cell*, *81*: 1137–1146, 1995.
53. Afti, A., Djelloul, S., Chastre, E., Davis, R., and Gespach, C. Evidence for a role of Rho-like GTPases stress-activated protein/c-Jun N-terminal kinase (SAPK/JNK) in transferring growth factor  $\beta$ -mediated signaling. *J. Biol. Chem.*, *272*: 1429–1432, 1997.
54. Talukder, A. H., Adam, L., Raz, A., and Kumar, R. Heregulin regulation of autocrine motility factor expression in human tumor cells. *Cancer Res.*, *60*: 474–480, 2000.